Melt Rheology and Morphology of Uncompatibilized and *In Situ* Compatibilized Nylon-6/Ethylene Propylene Rubber Blends

Zachariah Oommen,[1] Sisy R. Zachariah,[1] Sabu Thomas,[2] Gabriel Groeninckx,[2] Paula Moldenaers,[3] Jan Mewis[3]

[1]*Department of Criminal Justice, Albany State University, Albany, Georgia 31705*
[2]*Macromolecular Structural Chemistry, Department of Chemistry, Katholieke Universiteit of Leuven, Celestijnenlaan 200 F, B-3001, Heverlee, Belgium*
[3]*Department of Chemical Engineering, Katholieke Universiteit of Leuven, de Croylaan, 46, 3001, Heverlee, Belgium*

Received 11 February 2003; accepted 24 September 2003

ABSTRACT: Melt rheology and morphology of nylon-6/ethylene propylene rubber (EPR) blends were studied as a function of composition, temperature, and compatibilizer loading. Uncompatibilized blends with higher nylon-6 content (N90 and N95) and rubber content (N5 and N10) had viscosities approximately intermediate between those of the component polymers. A very clear negative deviation was observed in the viscosity–composition curve over the entire shear rate range studied for blends having composition N30, N50, and N70. This was associated with the interlayer slip resulting from the high-level incompatibility between the component polymers. The lack of compatibility was confirmed by fracture surface morphology, given that the dispersed domains showed no sign of adhesion to the matrix. The phase morphology studies indicated that EPR was dispersed as spherical inclusions in the nylon matrix up to 30 wt % of its concentration. A cocontinuous morphology was observed between 30 and 50 wt % nylon and a phase inversion beyond 70 wt % nylon. Various models based on viscosity ratios were used to predict the region of phase inversion. Experiments were also carried out on *in situ* compatibilization using maleic anhydride–modified EPR (EPR-*g*-MA). In this reactive compatibilization strategy, the maleic anhydride groups of modified EPR reacted with the amino end groups of nylon. This reaction produced a graft copolymer at the blend interface, which in fact acted as the compatibilizer. The viscosity of the blend was found to increase when a few percent of modified EPR was added; at higher concentrations the viscosity leveled off, indicating a high level of interaction at the interface. Morphological investigations indicated that the size of the dispersed phase initially decreased when a few percent of the graft copolymer was added followed by a clear leveling off at higher concentration. © 2004 Wiley Periodicals, Inc. J Appl Polym Sci 92: 252–264, 2004

Key words: rheology; morphology; compatibilization; nylon; ethylene propylene rubber (EPR)

INTRODUCTION

In recent years blending of polymers has gained importance as an alternative for developing new materials with good performance because of the possibility it offers of tailoring the individual properties in a single material. Thermoplastic elastomers from blends of rubbers and plastics have received considerable interest, and the required type of properties can be easily achieved by carefully selecting the component polymers and their blend ratio. The optimization of the melt-processing conditions is an essential step in controlling the microstructure and the ultimate properties of the final blend product. The influence of processing conditions on the morphology and properties has been the subject of several investigations.[1,2]

Only few polymers are miscible on a molecular level and most of the polymer pairs are immiscible and incompatible. This leads to poor mechanical properties. The final physical properties of immiscible polymer blends depend not only on the constituent polymers but also on the morphologies of the blends. A fine morphology can be achieved by controlling the interfacial tension, the ratio of viscosity of the components, and the processing conditions. The compatibility between immiscible polymers can be enhanced through the addition of compatibilizers. Compatibility may also be enhanced through the addition of low molecular weight compounds that promote copolymer formation.[3–5] The *in situ* formed copolymer anchoring along the interface is more effective than the conventional compatibilizer in compatibilizing the blend. A suitably selected compatibilizer should reduce the interfacial tension between the component polymers, permit finer dispersion during mixing, provide stability against gross segregation, and result in improved interfacial adhesion. Xanthos and Dagli,[4]

Correspondence to: Z. Oommen (zoommen@asurams.edu).

Journal of Applied Polymer Science, Vol. 92, 252–264 (2004)

Brown,[6] and Liu et al.[7] all reviewed the interfacial coupling approach in polymer blends. The basic criterion for such an approach, based on a reactive compatibilizer, is that both constituents must possess certain necessary functional groups capable of reacting during melt processing. The reaction should produce graft or block copolymers at the interface with segments containing both blend components.

Processing and rheological properties of blends have also been of great interest to polymer technologists. Rheological and morphological behavior of blends of polycarbonate (PC) with ABS and polycarbonate with maleic anhydride–grafted ABS (MABS) were studied by Balakrishnan et al.[8] They prepared the blends by melt mixing using a single-screw extruder. The resulting morphology of the unmodified blends was shown to be a coarse dispersion, whereas the modified blends resulted in fine dispersion. The correlation between the flow behavior and the structural and mechanical properties of polyamide-6 blends containing liquid crystalline polymers was previously reported by Meng and Tjong.[9] Thomas and coworkers[10–14] reported on the rheological behavior of several thermoplastic elastomers and related the properties with the morphology. Degee et al.[15] studied the effect of polymethacrylic ionomers on the melt viscosity of polyamide.

There are a number of reports on the morphology and properties of blends based on nylon and nonpolar polymers such as polyolefins.[16–18] Polyamides have some interesting properties, but they are characterized by high water absorption and impact brittleness. The blending of polyamides with olefins or other nonpolar polymers should be very promising for decreasing water absorption and improving impact strength. Recently, Thomas and Groeninckx[19] reported on the morphology development in a nylon-6/EPR blend (both compatibilized and uncompatibilized) prepared in a corotating twin-screw, miniextruder. Recently the morphology development by reactive compatibilization and dynamic vulcanization of nylon-6/EPDM blends with higher rubber fraction was discussed by Oderkerk and Groeninckx.[20] Very recently the melting and crystallization behaviors of nonreactive and reactive melt-mixed blends of polypropylene and carboxylic-modified polyamides in the dispersed phase were investigated by Gisela et al.[21] It was found that the size of the polyamide particles changes in dependency on mixing time of the blends. The investigations showed that the effect of fractionated crystallization can be used to follow the morphology development and to evaluate the efficiency of compatibilizing interfacial reactions during processing. The influence of screw speed, agitator configuration, and compatibilizer, during twin-screw extrusion, upon morphology and properties was investigated very recently by Tabtiang et al.[22] Although the morphology of nylon-6/EPR blends has been investigated, the rheological behavior in both the presence and the absence of compatibilizer is still not well understood.

TABLE I
Molecular Weight and the Materials Used

Materials	Source	MW
EPR (78% of ethylene)	Exxon	80,000
EPR-*g*-MA (0.6 wt % MA)	Exxon	80,000
Nylon-6	DSM	24,000

The main objective of the present study was to investigate the rheological properties of nylon-6/EPR blends as a function of composition, compatibilizer content, and processing conditions. An *in situ* reactive compatibilization technique was used to compatibilize the blends. The morphology of the extrudates was investigated by scanning electron microscopy studies and the size of the dispersed phase was evaluated by image analysis.

EXPERIMENTAL

Materials and blending procedure

Nylon-6 was supplied by DSM (Heerlen, The Netherlands) and the ethylene propylene rubber (EPR) and maleic anhydride–modified rubber (EPR-*g*-MA) were supplied by Exxon Chemical Company (Baytown, TX). The molecular weight of these materials is given in Table I. The blends of nylon-6/EPR over the whole composition range were prepared in a Haake Rheocord mixer (Haake, Bersdorff, Germany) at a temperature of 250°C and a fixed rotational speed of 100 rpm for 4 min. First the nylon was dried at 80°C for 24 h. The blends are denoted by N*x*, where N indicates nylon-6 and the digit *x* indicates wt % nylon in the blend. Reactively compatibilized blends having composition N30 and N70 with 0, 1, 2.5, 5 and 10 wt % compatibilizer loading were also prepared in the Haake mixer. The mixing conditions were the same as those of the uncompatibilized blends.

Rheological measurements

The viscosity of the component polymers and the blends was measured using a Gottfert capillary rheometer (Model 2002). Capillaries of L/D ratio 30, 20, and 10 were used, and the shear rates investigated ranged from 5 to 300 s^{-1}. The melt was extruded through the capillary at predetermined plunger speeds after a warm-up period of 5 min. The measurements were performed at a temperature of 250°C. Capillaries having an L/D ratio of 30/1, 20/1, and 10/1 were used to make Bagley plots. Also, the Rabi-

nowitch correction was applied to all experimental data.

The true wall shear rate $\dot{\gamma}_w$ was calculated from the apparent wall shear rate $\dot{\gamma}_{wa}$ by means of the following equation:

$$\dot{\gamma}_w = (3n + 1)/4n\dot{\gamma}_{wa} \quad (1)$$

where n, the flow index, is defined as

$$n = d(\log \tau_w)/d(\log \dot{\gamma}_{wa}) \quad (2)$$

where τ_w is the wall shear stress.

Morphology analysis

The morphology of the fracture surface of all blends was analyzed by means of scanning electron microscopy. The specimens were fractured in liquid nitrogen and the minor phase was extracted with a suitable solvent (boiling xylene for EPR and formic acid for nylon), dried at 80°C in a vacuum oven, and gold coated before SEM examination. The dispersed phase size was measured using an automatic image analyzing technique, which used imaging software. The diameter was measured by scanning the micrograph and individually outlining the particles to calculate the dimensions. Typically over 500 particles and several fields of view were analyzed, size-corrected for the fact that not all droplets were cut through the center. The number-average diameter (D_n) and weight-average diameter (D_w) were calculated from the following relationships:

$$D_n = \sum n_i D_i / \sum n_i \quad (3)$$

$$D_w = \sum n_i D_i^2 / \sum n_i D_i \quad (4)$$

where n_i is the number of particles of size i.

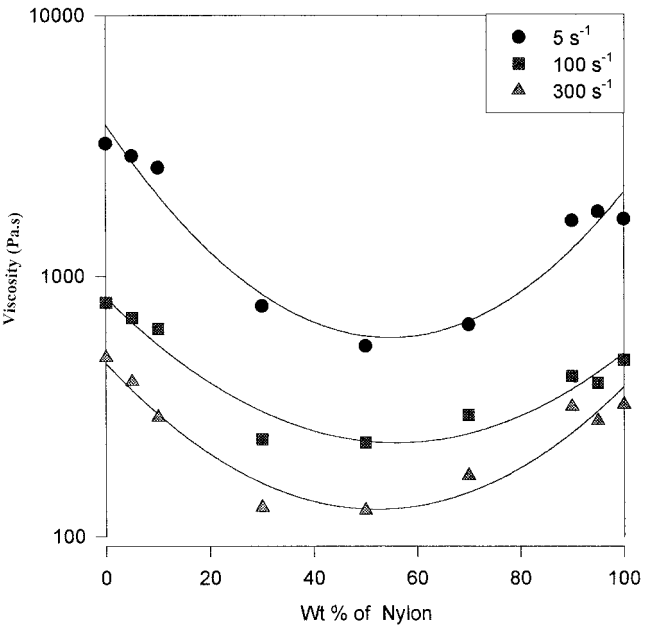

Figure 2 Viscosity as a function of wt % of nylon-6 in nylon-6/EPR blends at 50, 100, and 300 s^{-1}.

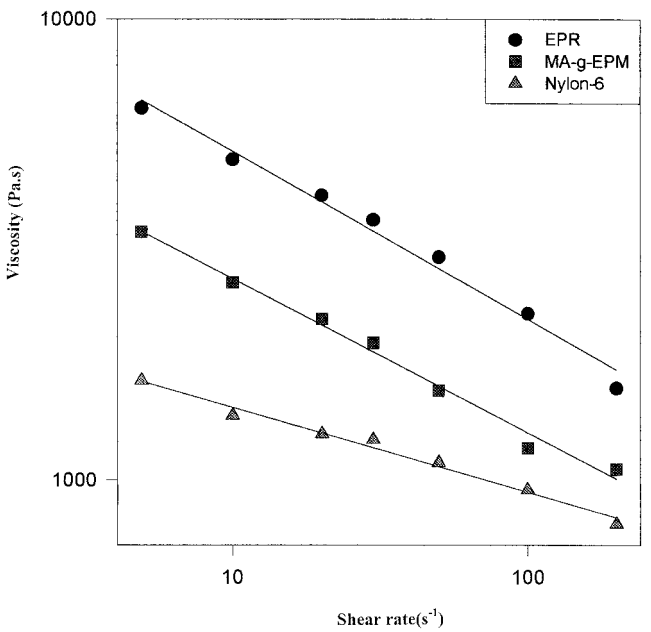

Figure 1 Viscosity as a function of shear rate of nylon-6, EPR, and EPR-*g*-MA.

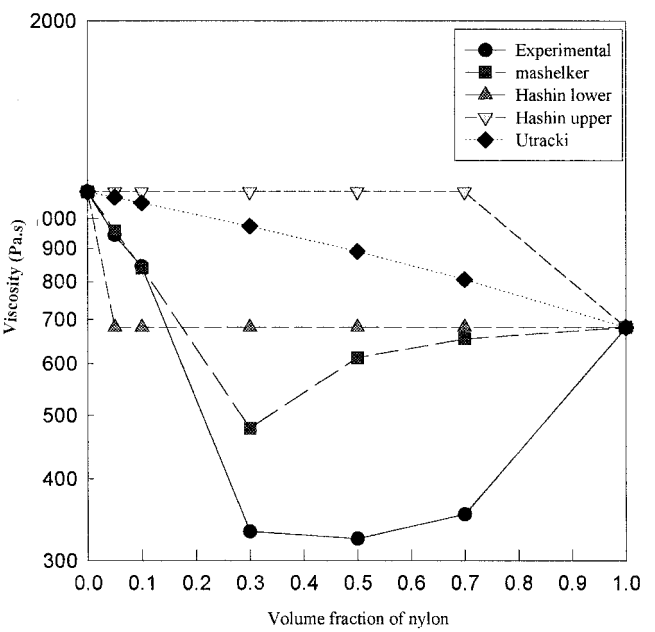

Figure 3 Comparison of experimental viscosity values with the calculated values from existing models.

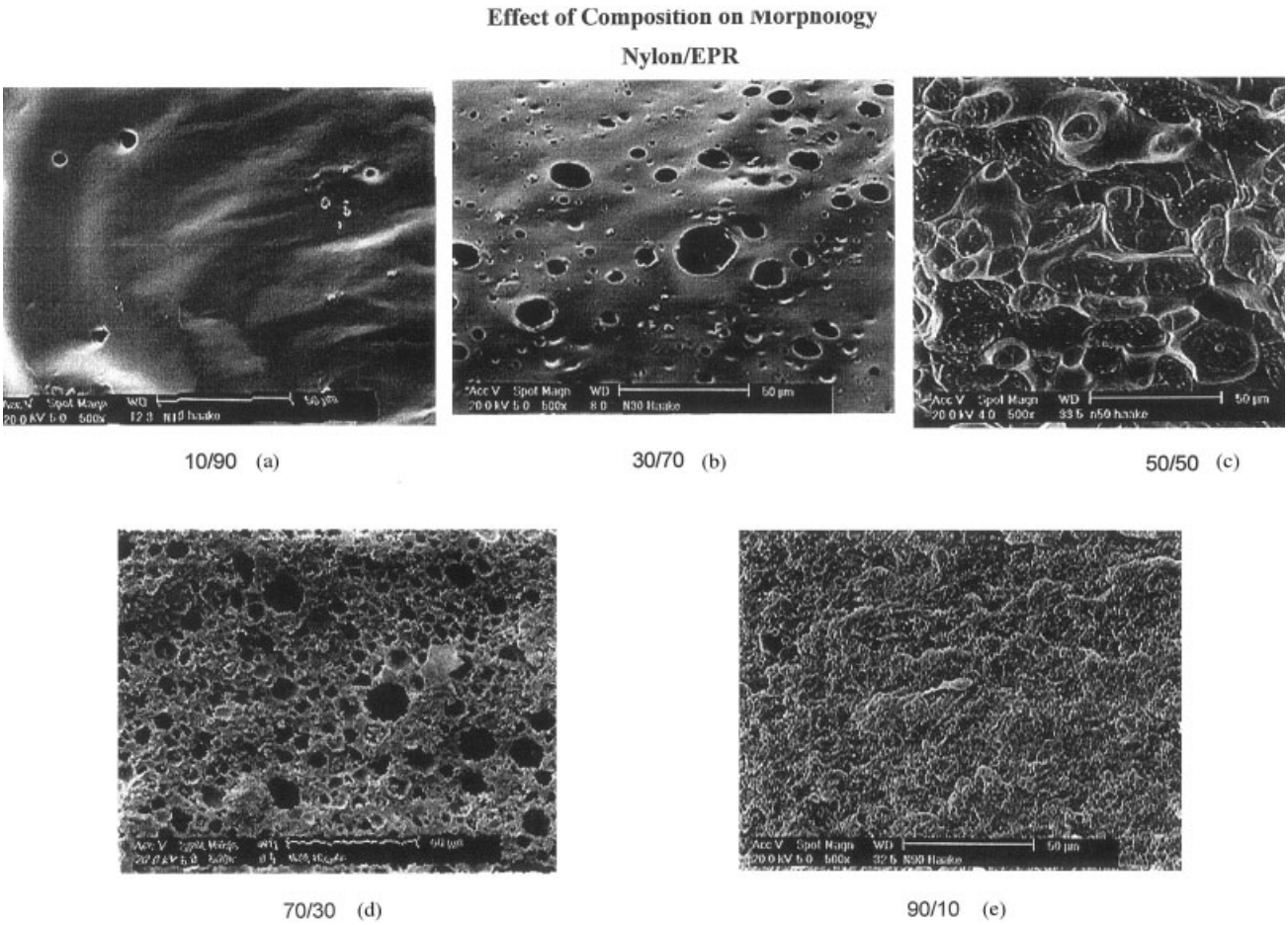

Figure 4 SEM micrographs of uncompatibilized nylon-6/EPR blends: (a) 10/90, (b) 30/70, (c) 50/50, (d) 70/30, and (e) 90/10.

RESULTS AND DISCUSSIONS

Rheology of uncompatibilized systems

The flow curves of the homopolymers nylon-6, EPR, and EPR-*g*-MA are given in Figure 1. The plots show the characteristic shear thinning behavior of molten polymers. The viscosity of EPR is about three times the viscosity of the polyamide for the lower shear rates. This ratio decreases with increasing shear rate because nylon is less shear thinning than EPR. The viscosity of graft copolymer is intermediate between that of nylon-6 and EPR. The component polymers were subjected to the same processing conditions as the blends. The torque measurements in the Haake mixer indicated the highest viscosity for EPR rubber. The N5 and N10 blends have viscosities approximately intermediate between those of nylon-6 and EPR. To obtain a more precise picture of the variation of viscosity with concentration at various shear rates some of the data are shown in Figure 2. The viscosities of the blends having composition N30, N50, and N70 are lower than those of the component polymers. Utracki and Sammut[23] studied in detail the variation of viscosity in polymer blends. According to these authors

$$\ln \eta_{i\,\text{app blend}} = \sum w_i \ln(\eta_{\text{app}})_I \tag{5}$$

where w_i is the weight fraction of the ith component of the blend and η_i is its viscosity. An immiscible blend can exhibit three types of behavior: positive deviation, as in a homogeneous blend in which there is a large interaction between the phases; negative deviation, when the interaction is small; and a positive–negative deviation, when there is a concentration-dependent change of structure. In two-phase polymer blends, the viscosity depends not only on the characteristics of the components but also on interfacial thickness and interfacial adhesion. The blends under considerations exhibited a negative deviation throughout the whole range of composition. One of the possible explanations for this behavior is a lack of adhesion between the segregated domains of the two components resulting in interlayer slip. A series of mixing rules were suggested to calculate the viscosity of the biphasic system. According to Hashin's upper and lower limit models, for heterogeneous materials[24]

$$\eta_{\text{mix}} = \eta_2 + \frac{\phi_1}{1/(\eta_1 - \eta_2) + \phi_2/2\eta_2} \tag{6}$$

$$\eta_{mix} = \eta_1 + \frac{\phi_2}{1/(\eta_2 - \eta_1) + \phi_1/2\eta_1} \quad (7)$$

where ϕ_i is the volume fraction of phase i. An altered free volume state model developed by Mashelkar and coworkers[25] was also applied to our system.

According to this model,

$$\ln \eta_{mix} = \frac{\phi_1(\alpha - 1 - \gamma\phi_2)\ln \eta_1 + \alpha\phi_2(\alpha - 1 + \gamma\phi_1)\ln \eta_2}{\phi_1(\alpha - 1 - \gamma\phi_2) + \alpha\phi_2(\alpha - 1 + \gamma\phi_1)} \quad (8)$$

where $\alpha = f_2/f_1$; $\gamma = \beta/f_1$; f_2 and f_1 are free volume fractions of components 1 and 2, respectively; and β is an interaction parameter.

$$f = 0.025 + \alpha_f(T - T_g)$$

$$\alpha_f = B/2.303C_1C_2$$

where $B \sim 1$, $C_1 = 17.44$, and $C_2 = 51.6$.

For the calculations, the value of γ was varied to obtain the best fit of the experimental results. The measured viscosities at a shear rate of 50 s^{-1} were found to be lower than those derived from the different mixing rules, as shown in Figure 3. Mixing rules without any negative interaction parameter cannot predict values for the blends that are lower than those for the components.

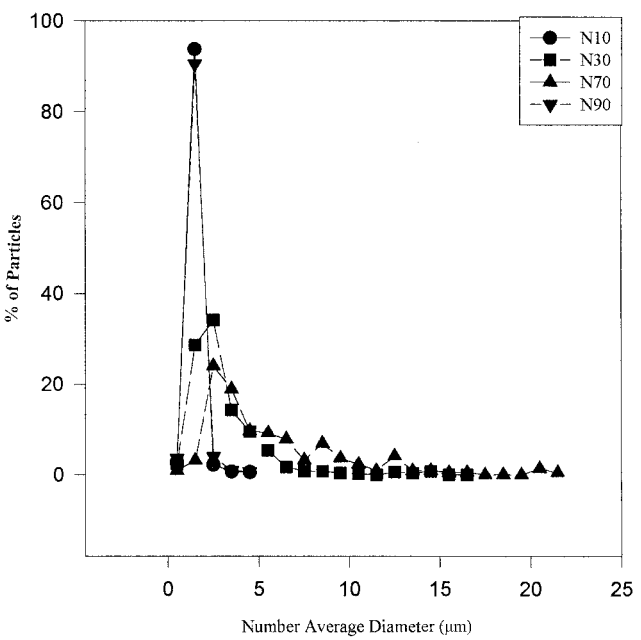

Figure 5 Domain size distribution of uncompatibilized nylon/EPR blends N10, N30, N70, and N90.

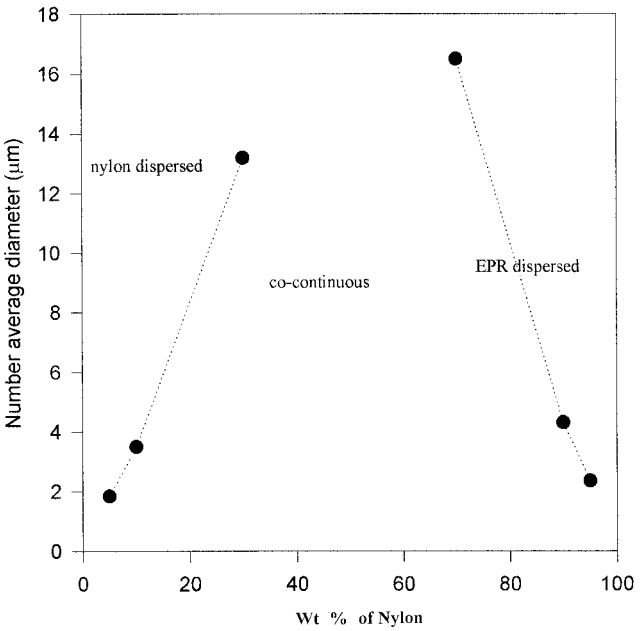

Figure 6 Number-average diameter as a function of composition of nylon/EPR blends.

Morphology of the uncompatibilized blend

Melt-blended immiscible polymer blends possess a complicated phase morphology that depends on interfacial tension, volume fraction, and viscosity ratio of the components and processing conditions. The final droplet size in a dilute blend after processing results from a balance between two forces: shear stresses, which tend to deform and rupture the particle; and interfacial stresses, which tend to resist this.[26,27] The results can be expressed in terms of the dimensionless capillary number Ca when the components are Newtonian.

$$\mathrm{Ca} = \eta_m\dot{\gamma}D/2\sigma \quad (9)$$

where η_m is the viscosity of the matrix, σ is the interfacial tension, D is the diameter, and $\dot{\gamma}$ is the shear rate.

The final morphology of a polymer blend with finite volume fraction of the components was determined by a competition between breakup and coalescence of the domains. In that case the final size tends to become larger with increasing concentration. At the same time the morphology becomes more complex depending on the details of the shear history.

The morphology of nylon-6/EPR blends with various compositions is shown in Figure 4(a)–(e). Nylon-6 is dispersed as spherical domains in blends with up to 30 wt % nylon-6. The domain size increases as the volume fraction of nylon in the blend increases. In N50 [Fig. 4(c)] a fibrillar phase appears. This morphology corresponds to the region of phase inversion, that is,

TABLE II
Predictions of Phase Inversion Point

Shear rate (s^{-1})	η_{Nylon}/η_{EPR}	Predicted weight fraction of EPR at which cocontinuity occurs			
		Paul and Barlow	Metelkin and Blekht	Chen-Su model	Ho model
5	0.51	0.38	0.90	0.59	0.56
10	0.57	0.41	0.85	0.59	0.57
20	0.59	0.41	0.84	0.58	0.57
30	0.55	0.40	0.86	0.59	0.57
50	0.62	0.43	0.81	0.58	0.58
100	0.60	0.42	0.83	0.58	0.57
200	0.63	0.43	0.81	0.58	0.58
300	0.66	0.45	0.78	0.58	0.58

the region of cocontinuous phases. The increase in the domain size of the dispersed nylon-6 phase with increase in concentration of the nylon-6 is associated with the coalescence of the drops. As coalescence increases drops become progressively larger and more deformed, ultimately producing fibrils.[28–30] This is in agreement with the studies of Danesi and Porter.[28] After the phase inversion, we can once more observe a spherical morphology now made of EPR particles. In Figure 4(d) where nylon-6 is 70 wt %, we can observe holes of the EPR domains extracted by the solvent. When EPR is the dispersed phase, the size of the domains is again spherical but coarser and larger than the nylon-6 domain of the same concentration. This is associated with the high viscosity of the rubber phase, which resists the agglomeration of nylon domains. In fact, when the matrix phase is more viscous, the higher shear forces and hence the decreasing collision times along with a more difficult matrix interlayer film drainage between the colliding droplets reduce the probability for coalescence. So it is clear that coalescence is more predominant in the case of the dispersed EPR phase in the low-viscosity nylon-6 matrix.

The distribution of the domains was quantified by image analysis. The domain size distribution curves of the blends as a function of composition are given in Figure 5. The blends N10 and N90 show a narrow distribution, whereas N30 and N70 show a broad one. The figure clearly indicates that the particle size distribution becomes wider with an increase in the dispersed phase concentration. This can be associated with the dynamic equilibrium between breakup and coalescence in more concentrated systems. The number-average diameter is plotted as a function of composition in Figure 6. The results are in agreement with the discussion in the previous paragraph. The EPR domain size is larger than that of nylon-6 at the same

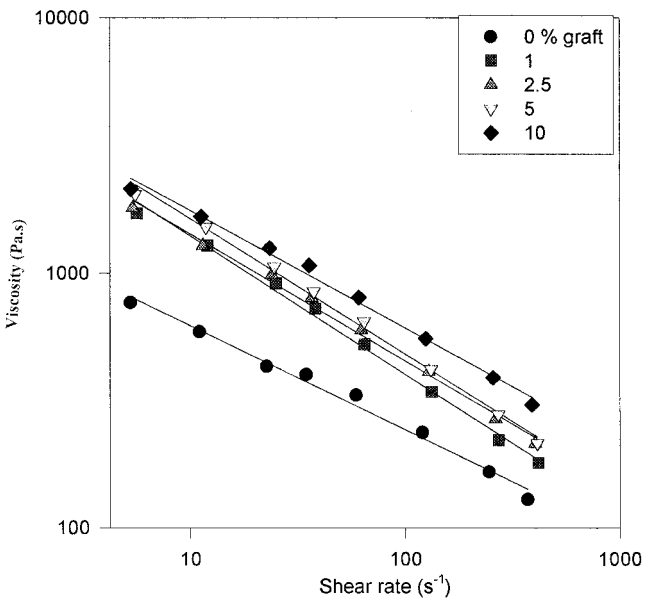

Figure 7 Viscosity as a function of shear rate of compatibilized nylon-6/EPR blends. N30 with 0, 1, 2.5, 5, and 10 wt % graft copolymer.

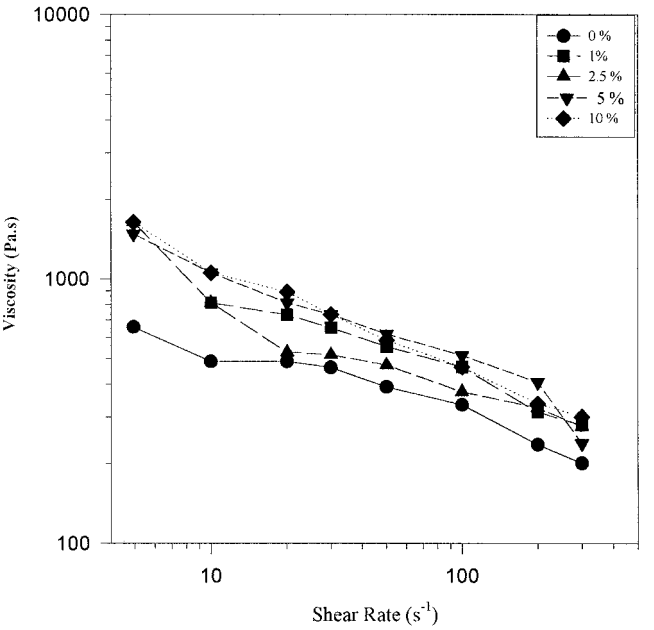

Figure 8 Viscosity as a function of shear rate of compatibilized nylon-6/EPR blends. N70 with 0, 1, 2.5, 5, and 10 wt % graft copolymer.

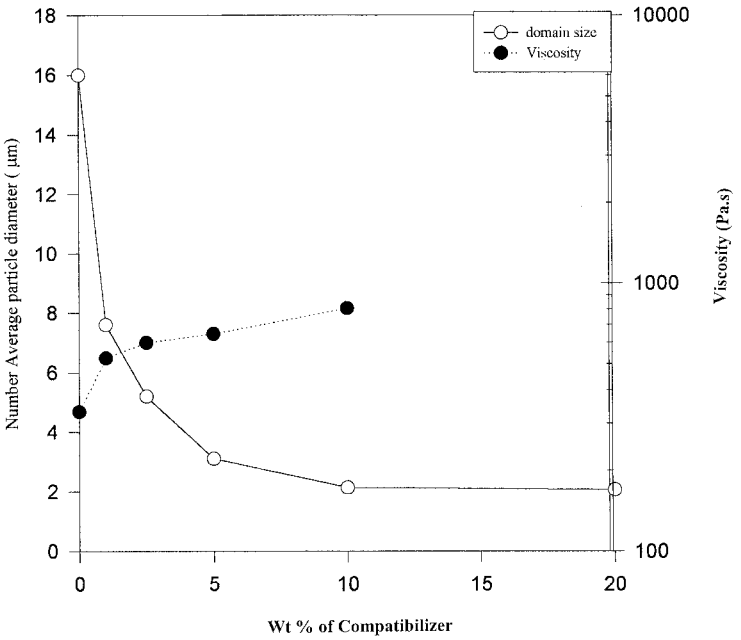

Figure 9 Number-average diameter and viscosity as a function of wt % of compatibilizer.

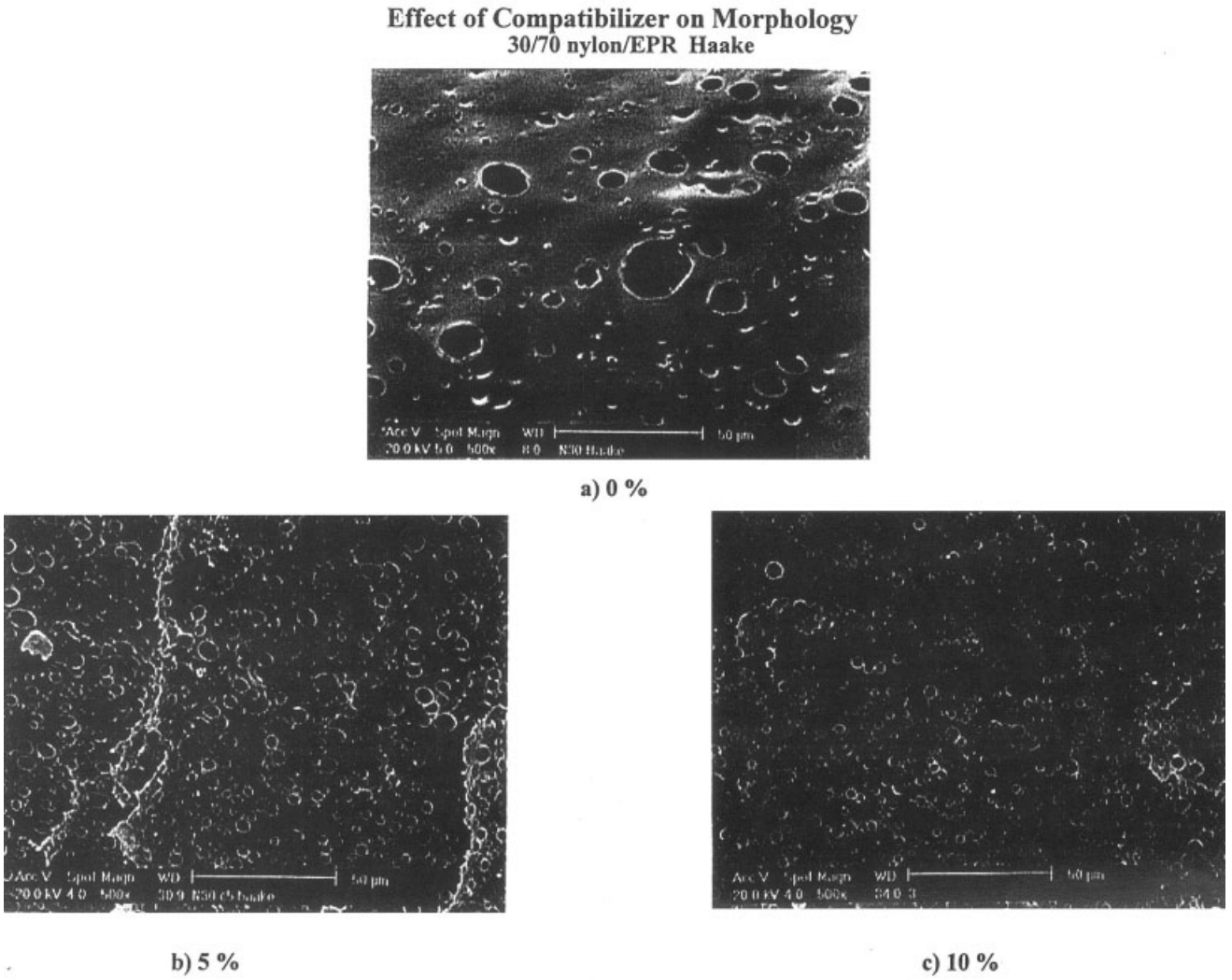

Figure 10 SEM micrographs of 30/70 nylon-6/EPR blend as a function of compatibilizer loading: (a) 0, (b) 5, and (c) 10 wt % graft copolymer.

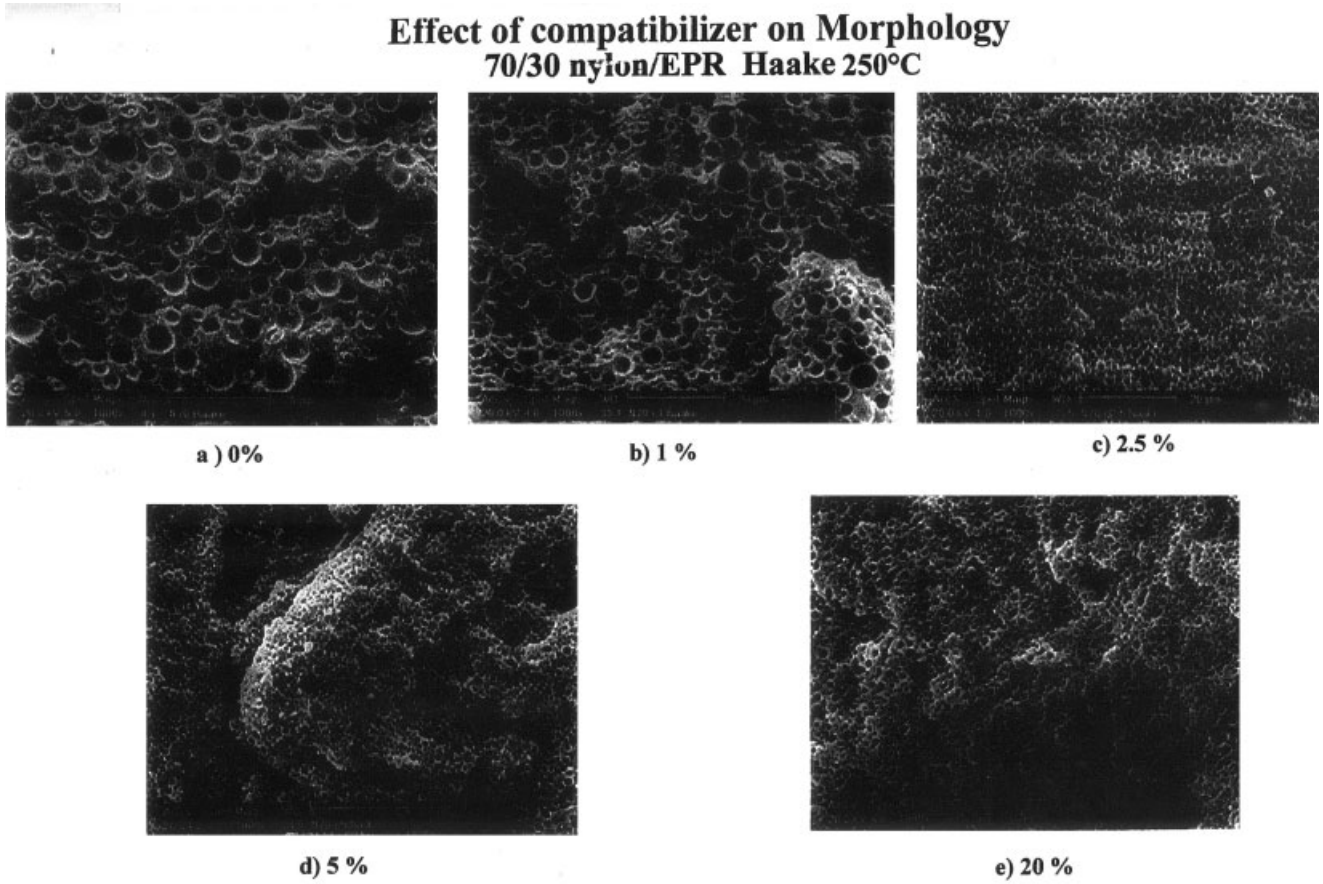

Figure 11 SEM micrographs of 70/30 nylon-6/EPR blend as a function of compatibilizer loading: (a) 0, (b) 1, (c) 2.5, (d) 5, and (e) 20 wt % graft copolymer.

volume fraction, which is explained on the basis of the effect of matrix viscosity on the coalescence. With the more viscous EPR as the matrix phase, drainage of the matrix filler interlayer between colliding droplets become more difficult, thus reducing coalescence.

Region of phase inversion

A change in composition or viscosity ratio has a marked effect on the location of the region of phase inversion. Several empirical relations have been proposed in the literature, to describe the point of phase inversion. Paul and Barlow[31] and Jordhamo et al.[32] reported an empirical model based on the melt viscosity and the volume fractions. According to these authors the phase-inversion point is given by

$$\phi_1/\phi_2 = \eta_1(\dot{\gamma})/\eta_2(\dot{\gamma}) \tag{10}$$

where the viscosities are taken at the shear rate of blending. This equation, however, is limited to low shear rates, and does not account for the effect of interfacial tension between phases. Nevertheless, this equation gives a good indication to shift the phase inversion of a polymer blend.

Chen and Su[33] proposed an equation

$$\phi_{hv}/\phi_{lv} = 1.2(\eta_{hv}/\eta_{lv})^{0.3} \tag{11}$$

where hv and lv denote the high- and low-viscosity phase, respectively. Chen and Su explained the asymmetry as a result of postmixing coarsening, which depends more heavily on the matrix viscosity, an effect that will be more pronounced at compositions rich in the low-viscous phase. Ho et al.[34] correlated these data with a relation between volume fraction and torque ratio, where they assumed the torque ratio and viscosity ratio to be equal.

$$\phi_1/\phi_2 = 1.22[\eta_1(\dot{\gamma})/\eta_2(\dot{\gamma})]^{0.29} \tag{12}$$

Metelkin and Blekht[35] used the theory of Tomotika[36] to describe the phase inversion in polymer blends. Their model is based on the instability of a liquid cylinder surrounded by another liquid. The resulting equation is then

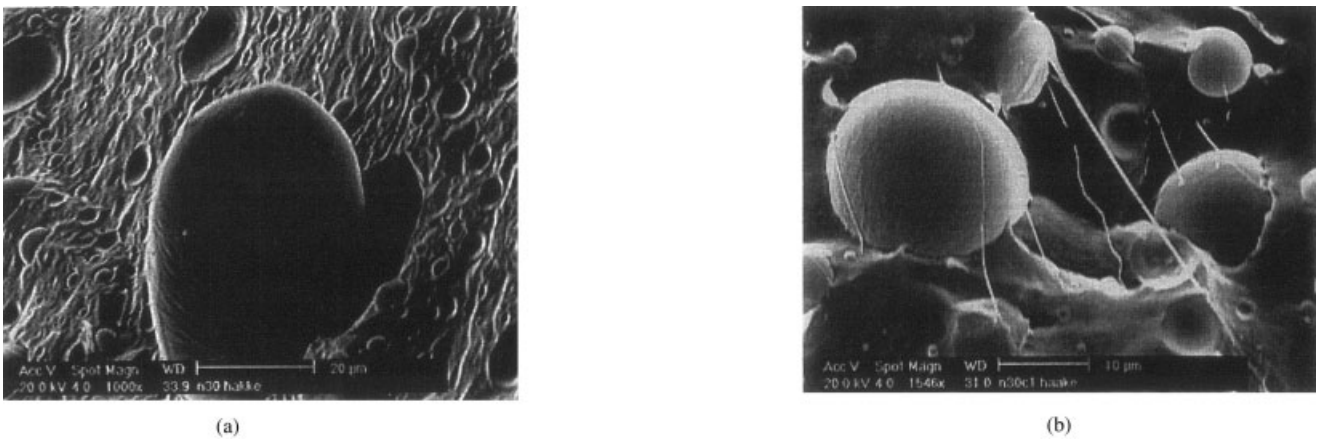

Figure 12 SEM micrographs of 30/70 nylon-6/EPR blend as a function of compatibilizer loading: (a) 0 and (b) 1 wt % graft copolymer.

$$\phi_1 = [1 + \eta_1/\eta_2(1 + 2.25 \log \eta_1/\eta_2 + 1.81(\log \eta_1/\eta_2)^2)]^{-1} \quad (13)$$

The predicted phase-inversion points calculated from eqs. (11)–(13), using viscosities obtained in the shear rate range from 5 to 300 s^{-1}, are given in Table II. The phase-inversion region calculated from the above models is not able to make a correct prediction of the composition range. According to the phase morphology by SEM the phase inversion takes place between 30 and 70 wt % of nylon-6 or rubber.

Rheology of reactively compatibilized blends

The addition of compatibilizer to polymer blends affects the flow behavior because it changes the interaction of the components at their interface. The viscosity of a polyamide/polypropylene blend was found to increase when compatibilized with maleic anhydride grafted styrene–(ethylene-*co*-butylene)–styrene copolymer (SEBS-*g*-MA), as a consequence of chemical reactions occurring between amine and anhydride groups.[37,38] Germain and Genelot[39] reported that the addition of copolymer increases the dynamic viscosity of polypropylene/polyamide-6 blends. Similar results were also reported by Nishio et al.[40]

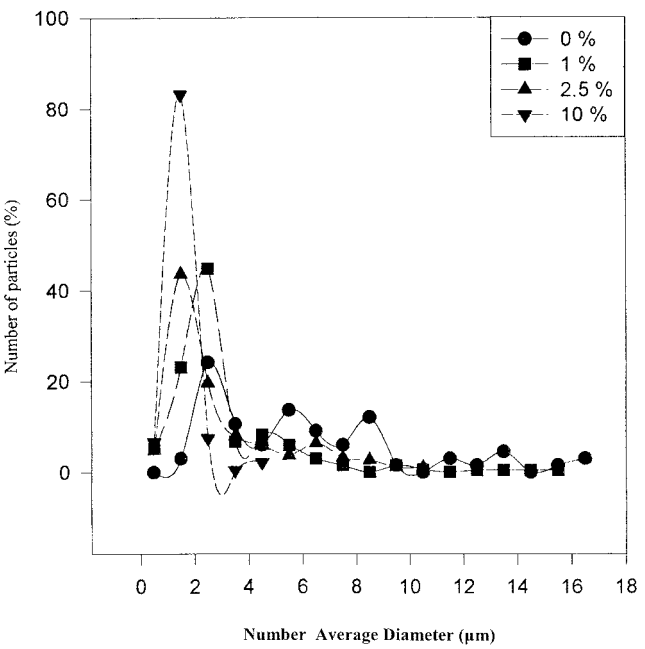

Figure 13 Domain size distribution of 30/70 nylon-6/EPR blend as a function of compatibilizer loading.

Here we report on the influence of reactive blending on the rheological behavior of nylon/EPR blends. In Figures 7 and 8 flow curves are displayed for the 30/70 and 70/30 nylon-6/EPR blends, respectively, with and without compatibilizer. The effect of compatibilization is quite significant. The viscosity increased with compatibilizer loading. Figure 9 shows the variation of viscosity as a function of compatibilizer loading. With increasing compatibilizer a leveling off at higher loadings follows loading the initial increase in viscosity, which is an indication of the interfacial saturation. The mechanism of compatibilization by the addition of maleic modified rubber to nylon-6/EPR blends can be explained as follows. Initially the modified rubber EPR-*g*-MA reacts with nylon-6, forming the graft copolymer EPR–MA-*g*-nylon. The newly formed compatibilizer locates at the interface between the nylon and the rubber. Interfacial location is shown in the following schematic:

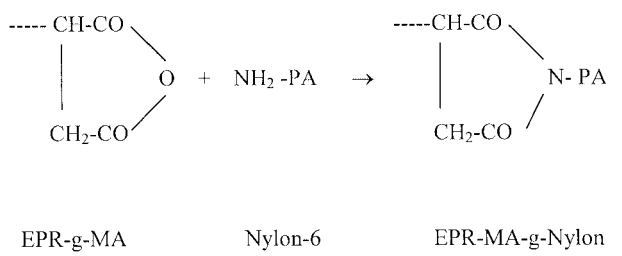

The graft copolymers formed at the interface increase the interfacial friction under shear stress. The graft

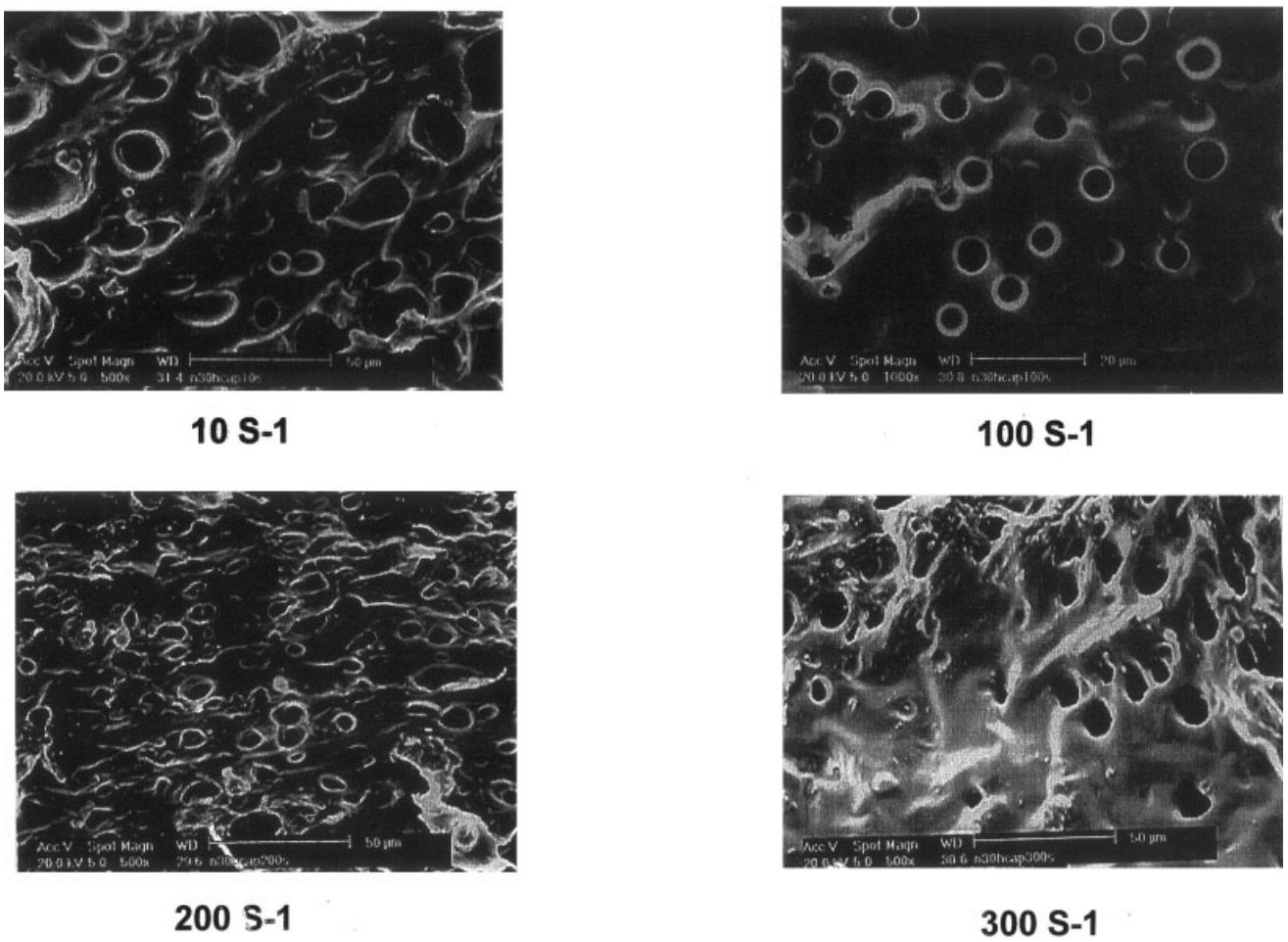

Figure 14 SEM micrographs of uncompatibilized nylon-6/EPR blends as a function of shear rate at 10, 100, 200, and 300 s^{-1}.

copolymer formed locates at the interface, leading to an increase in the interfacial thickness. This will result in effective stress transfer between the dispersed phase and the continuous phase and an increase in interfacial adhesion. This contributes to the reduction in interlayer slip and therefore to an increase in viscosity.

Morphology of reactively compatibilized blends

The morphology of the reactively compatibilized blends was followed as a function of compatibilizer concentration. Blends without compatibilizer exhibit dispersion morphology with spherical particles, at least outside the cocontinuity system. The interface is well defined, indicating weak interfacial adhesion between the dispersed and the matrix phases. The presence of compatibilizer significantly reduces the size of the dispersed phase and shows good interfacial adhesion. The effect of maleic-modified rubber as a reactive compatibilizer on the morphology of 30/70 nylon-6/EPR blend is demonstrated in the SEM micrographs of Figure 10(a)–(c). The compatibilized blends give more uniform and finer spherical particles of the dispersed phase. The particle diameter of the dispersed phase decreases as a function of compatibilizer loading, leveling off at about 5 wt % graft copolymer concentration. An increase in viscosity and a reduction in domain size when adding compatibilizer (Fig. 9) indicates that the maleic-modified rubber acts effectively as a reactive compatibilizer. The leveling off at both domain size and viscosity is an indication of interfacial saturation. The *in situ* formed graft copolymer tends to anchor along the interface, thus performing as an effective compatibilizer in the blend. The same trend can be seen in the morphology changes for the 70/30 nylon/EPR compatibilized blend [Fig. 11(a)–(e)]. Addition of compatibilizer beyond the critical concentration will lead to micelle formation. Sundararaj and Macosko[41] showed that formation of micelles in PS/PMMA blends occurs when the concentration of PS-*co*-PMMA diblock copolymer becomes larger than 1–2 wt %. The critical concentration for micelle formation depends on the structure and the molecular weight of the copolymer.

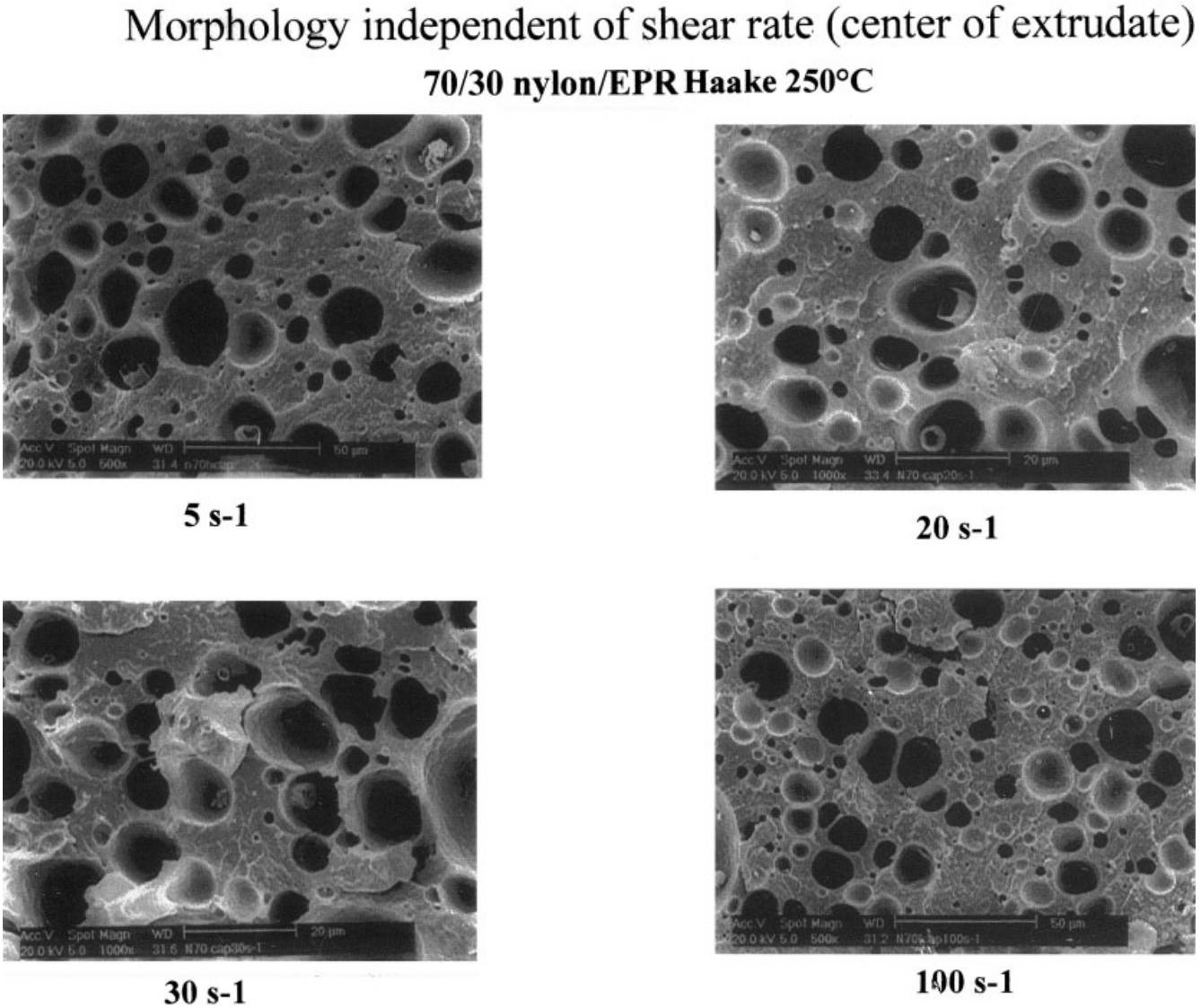

Figure 15 SEM micrographs of uncompatibilized nylon-6/EPR blends as a function of shear rate at the center of the extrudate.

The interfacial bonding upon compatibilization can be deduced from the SEM micrographs of the fracture surface of 30/70 nylon-6/EPR blend with 0 and 1 wt % of graft copolymer. In the blend with 0 wt % graft copolymer, nylon-6 domains show no sign of interfacial bonding. After the addition of even 1 wt % graft copolymer the adhesion between the phases increases and the formation of interfacial bonding is evident (Fig. 12). The domain size distribution curves of the 30/70 nylon-6/EPR blend compatibilized with different maleic-modified rubber loading are given in Figure 13. The uncompatibilized blend shows a broader distribution curve, with a nonuniform distribution of nylon domains. As the compatibilizer loading increases the curves become narrower and the size decreases. This can be explained based on two factors. As mentioned earlier, suppression of coalescence attributed to the formation of compatibilizer shell around the dispersed phase and the reduction in interfacial tension are considered the major mechanisms contributing to these effects.

The morphology of the extrudate collected after the capillary viscosity measurements was also examined. Scanning was performed on the periphery as well as on the center of the extrudate and then at various shear rates. The SEM micrographs of the uncompatibilized 30/70 nylon-6/EPR blend as a function of shear rate are shown in Figure 14. The domain size of the dispersed nylon phase decreases with increasing shear rate at the periphery of the extrudate. At the center of the extrudate, where the shear rate is essentially zero domain size, remains unchanged (Fig. 15). For compatibilized blends the domains are almost the

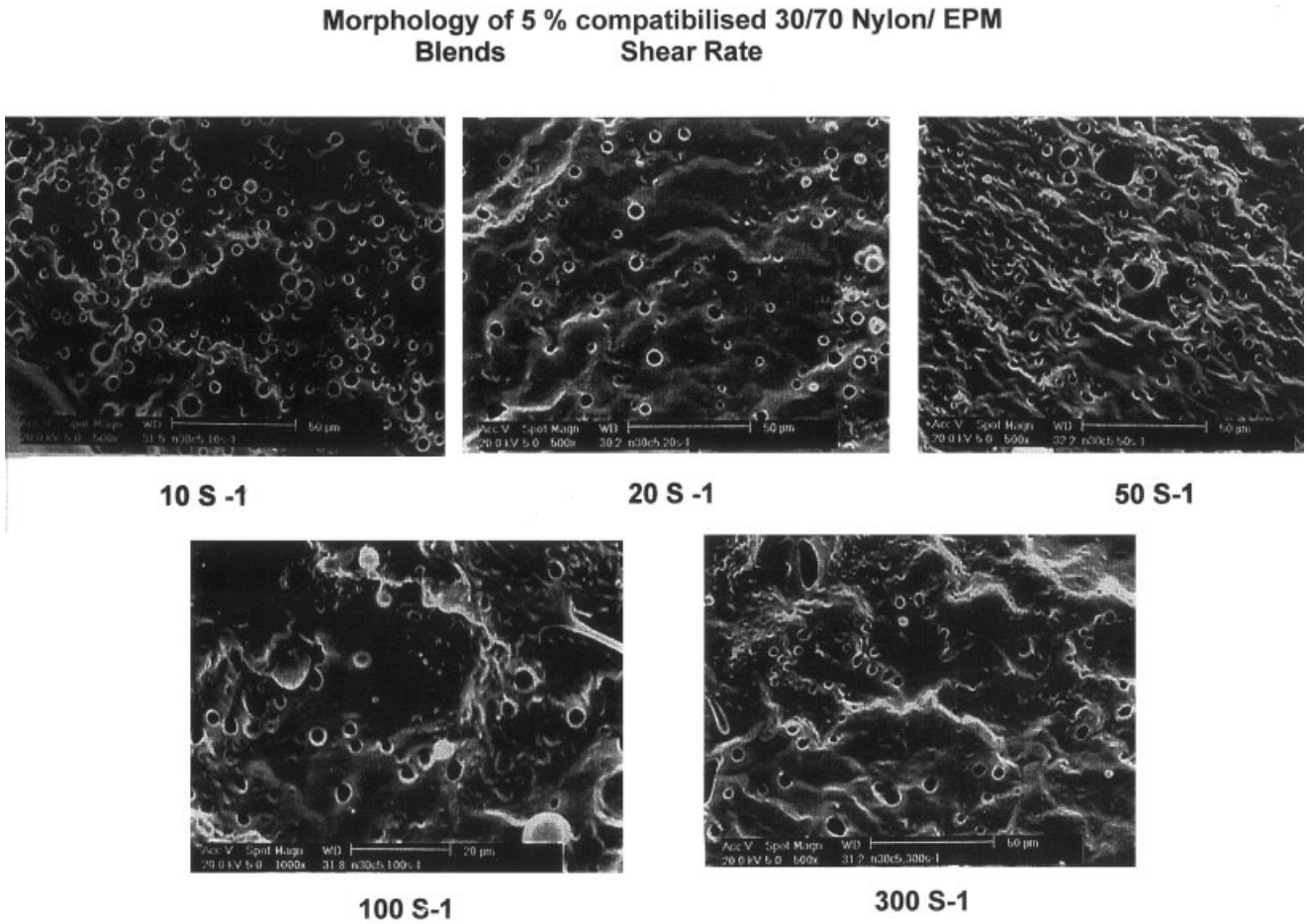

Figure 16 SEM micrographs of 5 wt % compatibilized nylon-6/EPR blends as a function of shear rate.

same in the periphery and at the center of the extrudate irrespective of the shear rates (Fig. 16). The lack of a shear rate effect on the morphology confirms the stability of the compatibilized blends.

CONCLUSIONS

Melt rheology and morphology of uncompatibilized and reactively compatibilized nylon-6/EPR blends were investigated as a function of composition. The viscosity–composition curves show a well-defined negative deviation with some blend viscosities lower than those of the two components. Interlayer slip between the two phases is considered the major reason for the negative deviation.

The morphology of the blends was also examined over the entire range of composition. The domain size increases with increasing amount of dispersed phase (nylon-6 or EPR), attributed to coalescence effects. The size distribution becomes wide with increase in concentration of the dispersed phase, again because of a more pronounced coalescence. Fibrillar morphology in the case of 50/50 nylon/EPR blend is an indication of phase inversion.

Maleic anhydride–modified rubber was used to compatibilize nylon-6/EPR blends. The *in situ* formed compatibilizer, located at the interphase, reduced the interfacial tension, suppressing and enhancing the adhesion between the phases. As a consequence the domain size decreased with compatibilizer loading and leveled off at about 5 wt % compatibilizer. The domain size distribution also narrowed considerably with the addition of compatibilizer.

The effect of compatibilization on the rheology of blend was studied at various shear rates. The viscosity increased considerably with the addition of 1 wt % of EPM-*g*-MA, leveling off at higher concentrations of the copolymer. Contrary to the case of uncompatibilized blends the morphology of the compatibilized blends was quite stable with respect to changes in the shearing conditions.

References

1. Utracki, L. A. Polym Eng Sci 1996, 12, 36.
2. Scott, C. E.; Macosko, C. W. Polymer 1994, 35, 5422.
3. Mascia, L.; Xanthos, M. Adv Polym Technol 1992, 11, 237.
4. Xanthos, M.; Dagli, S. S. Polym Eng Sci 1991, 31, 929.

5. Chang, F. C. In: Compatibilized Thermoplastic Blends; Olabisi, O., Ed.; Handbook of Thermoplastics; Marcel Dekker: New York, 1997; Vol. 21, p. 491.
6. Brown, S. B. In: Reactive Extrusion; Xanthos, M., Ed.; Hanser: New York, 1992; Chapter 4.
7. Liu, W. B.; Kuo, W. F.; Chiang, C. R.; Chang, F. C. Eur Polym Mater 1996, 32, 91.
8. Balakrishnan, S.; Neelakantan, N. R.; Nabi Saheb, D.; Jog, J. P. Polymer 1998, 39, 5765.
9. Meng, Y. Z.; Tjong, S. C. Polymer 1998, 39, 99.
10. Oommen, Z.; Kuriakose, B.; Premalatha, C. K.; Thomas, S. Polymer 1997, 36, 5611.
11. George, S.; Joseph, R.; Varughese, K. T.; Thomas, S. Polymer 1995, 36, 4405.
12. George, J.; Thomas, S.; Varghese, K. T.; Ramamurthy, K. J. Polym Sci Phys Ed 2000, 38, 110.
13. Sobha, V. N.; Oommen, Z.; Thomas, S. J Appl Polym Sci 2002, 86, 3537.
14. Molly, K. A.; Oommen, Z.; Bhagawan, S. S.; Groeninckx, G.; Thomas, S. J Appl Polym Sci 2002, 86, 3210.
15. Degee, Ph.; Vankan, R.; Teyssie, Ph.; Jerome, R. Polymer 1997, 38, 3861.
16. Chang, F. C.; Hwu, Y. C. Polym Eng Sci 1991, 31, 1609.
17. Huitric, J.; Mederic, P.; Moan, M.; Jarrin, J. Polymer 1998, 39, 4849.
18. Asish, A. J.; Bhattacharyya, K.; Bhowmick, A. K. Polym Netw Blends 1997, **7**, 177.
19. Thomas, S.; Groeninckx, G. J Appl Polym Sci 1999, 28, 1405.
20. Oderkerk, J.; Groeninckx, G. Polymer 2002, 43, 2219.
21. Gisela, P.; Petra, P.; Jurgen, P. J Appl Polym Sci 2002, 86, 3445.
22. Tabtiang, A.; Venables, R. A. Polymer 2002, 43, 4791.
23. Utracki, L. A.; Sammut, P. Polym Eng Sci 1981, 28, 1405.
24. Hashin, Z. In: Second Order Effects in Elasticity, Plasticity, and Fluid Dynamics; Reiner, M.; Abir, S., Eds.; Macmillan: New York, 1964.
25. Sood, R.; Kulkarni, M. G.; Dutta, A.; Mashelkar, R. A. Polym Eng Sci 1988, 20, 28.
26. Plochocki, A. P.; Dagli, S. S.; Andrews, R. D. Polym Eng Sci 1990, 30, 741.
27. Fortelny, I.; Zivny, A. Polym Eng Sci 1995, 35, 1872.
28. Danesi, S.; Porter, R. S. Polymer 1978, 19, 448.
29. Heikens, D.; Barentsen, W. M. Polymer 1977, 18, 69.
30. Favis, B. D.; Chalifoux, J. P. Polymer 1988, 29, 1761.
31. Paul, D. R.; Barlow, J. W. J Macromol Sci Rev Macromol Chem C 1980, 18, 109.
32. G. M.; Jordhamo, J. A.; Manson, L. H. Sperling, Polym Eng Sci 1986, 26, 517.
33. Chen, T. H.; Su, A. C. Polymer 1993, 34, 4826.
34. Ho, R. M.; Wu, C. H.; Su, A. C. Polym Eng Sci 1990, 30, 511.
35. Metelkin, V. I.; Blekht, V. S. Colloid J USSR 1984, 46, 425.
36. Tomotika, S. Proc R Soc Lond A 1935, 150, 322.
37. Miettinen, R. H. M.; Seppala, J. V.; Ikkala, O. T.; Reima, I. T. Polym Eng Sci 1994, 34, 395.
38. Germain, Y.; Ernst, B.; Genelot, O.; Dhamini, L. J Rheol 1994, 38, 681.
39. Germain, Y.; Genelot, O. Rheological Analysis of Compatibilized PP/PA6 blends, PPS7; Hamilton, Canada, April 21–24, 1991.
40. Nishio, T.; Higashi, K.; Sanada, T.; Suzuki, Y.; Kakugo, M. Morphology Change and Flow Behaviour of Polyamide Alloy by Reactive Processing, PPS10; Akron, OH, April 5–8, 1994.
41. Sundararaj, U.; Macosko, C. W. Macromolecules 1995, 28, 2647.